Supporting Information

A Keggin-type polyoxomolybdate-based crystalline material formed by hydrothermal transformation: photo/electro-catalytic properties and mechanism study

Peisen Wang,‡[a] Aadil Nabi Chishti,‡[a] Peng Chen,[a] Zengxiang Lv,[a] Yaya Tan,[a] Hanzhi Zhang,[a] Junjie Zha,[a] Zhiyuan Ma,[a] Lubin Ni,*[a] Lu-nan Zhang*[a] and Yongge Wei*[bc]

[a] School of Chemistry and Chemical Engineering, Yangzhou University, Yangzhou 225002, China
E-mail: lbni@yzu.edu.cn, zhangln@yzu.edu.cn, yonggewei@mail.tsinghua.edu.cn
[b] Key lab of Organic Optoelectronics & Molecular Engineering of Ministry of Education, Department of Chemistry, Tsinghua University, Beijing 100084, China.
[c] State Key Laboratory of Natural and Biomimetic Drugs, Peking University, Beijing 100191, China.

‡These authors contributed equally to this work.

Experimental Section

1. Physical measurements

Fourier-transform infrared (FT-IR) spectra were obtained with a Cary 5000 FT-IR spectrometer using KBr particles in the range of 400-4000 cm^{-1}. Powder XRD (PXRD) patterns (2θ = 5-50°) were collected at room temperature using a Bruker D8 Advance XRD diffractometer at 40 kV and 40 mA with Cu Kα (λ = 1.5406 Å) radiation. Using a TG 209F3 thermogravimetric analyzer from the German Netzsch Group, under air atmosphere with a heating rate of 10 $K \cdot min^{-1}$ in the temperature region of 30-900 °C.

2. Single-crystal structure determination

Single crystal X-ray diffraction data of complex **1** were collected at 293 K using a sealed Tube Bruker Smart APEX II CCD (Mo Kα radiation, λ = 0.71073 Å). All the non-H atoms were determined by direct methods and refined anisotropically by full-matrix least-squares techniques based on F^2 by using the SHELXTL software package and Olex 2 software.[1,2] More details of X-ray structure analysis are given in **Table S1**. The selected bond lengths and angles are listed in **Table S2**.

3.Photocatalytic process

The photocatalytic process was proceeded in a water-cooling quartz container. 50 mg of complex **1** was dispersed in 100 mL of 10 mg L^{-1} MB aqueous solution and magnetically stirred for about 30 min to ensure the adsorption-desorption equilibrium in the dark. After the dark reaction, 500 μL of H_2O_2 was added into the above solution, and the mixture was exposed to a UV lamp with continuous stirring. 2.0 mL samples were collected after every 4 minutes and analyzed by using a UV-Vis spectrophotometer.

4.Electrochemical measurements

Electrochemical experiments were carried out using an electrochemical workstation (CHI760E, Chen Hua, China). A typical three electrode system was established: a modified glassy carbon working electrode (GCE, d = 3mm), a saturated calomel electrode (SCE) reference electrode, and a Pt wire counter electrode. The working electrode was prepared as follows: 4 mg of complex **1** and 1 mg of Ketjenblack carbon were dispersed in 1 mL of ethanol and thoroughly ground in a mortar. The mixture was completely transferred into a 1.5 mL centrifuge tube, to which 50 μL of Nafion solution (5 wt%) was added, and then the mixture was further sonicated for 1 h to ensure fully

dispersed. Afterward, 5 μL of the obtained homogeneous ink was dropped onto the surface of a bare GCE. Finally, the electrode was dried in the air.

Table S1. Crystallographic data and structural correction parameters.

Complex	**1**
Empirical formula	$C_{60}Cu_6SiMo_{18}N_{12}O_{62}$
Formula weight	4096.97
Temperature, K	293(K)
Wavelength, Å	Mo *Kα*(0.71073)
Crystal system	Monoclinic
Space group	*P21/c*
a, Å	13.9435(8)
b, Å	20.0147(12)
c, Å	17.2063(11)
α, °	90
β, °	93.972
γ,°	90
V, Å^3	4790.3(5)
Z	2
D (calculated), g/cm^3	2.840
Abs. coeff., mm^{-1}	3.695
F(000)	3848.0
Crystal size, mm	0.18 x 0.10 x 0.08
θ range for data collection, °	3.126 ~ 54.206
Reflections collected / unique / R_{int}	44626/10907/0.0486
Data / restraints / parameters	10471/0/739
GOF on F^2	1.156
Final R indices R_1, wR_2 [$I > 2\sigma(I)$]	0.0674, 0.1617
R indices R_1, wR_2 [all data]	0.0766, 0.1665
Largest diff. peak and hole, e. Å^{-3}	2.00 /-1.53

$R_1 = \sum(Fo - Fc)/\sum Foand\ wR_2 = \{\sum w(Fo^2 - Fc^2)^2/\sum w(Fo^2)^2\}^{1/2}$

Table S2. Selected bond lengths (Å) and selected angles (º) for complex **1**.

Mo(1)-O(24)	1.728(8)	Mo(1)-O(29)[1]	2.131(6)
Mo(1)-O(25)	1.772(7)	Mo(1)-O(27)[1]	2.186(7)
Mo(1)-O(23)	1.773(7)	Mo(1)-O(28)	2.219(7)
Cu(1)-O(25)	1.924(7)	Cu(2)-O(30)	1.974(7)
Cu(1)-O(26)	1.980(7)	Cu(3)-O(23)	1.932(7)
Cu(1)-N(3)	1.979(9)	Cu(3)-O(22)	1.942(7)
Cu(1)-N(4)	1.983(9)	Cu(3)-N(2)	1.985(8)
Cu(1)-O(32)[1]	2.417(7)	Cu(3)-N(1)	1.988(9)
Cu(2)-O(31)	1.917(7)	Cu(3)-O(8)	2.375(9)
Cu(2)-N(5)	1.970(9)	Si (1)-O(11)[2]	1.638(14)
Si(1)-O(3)[2]	1.596(14)	Si (1)-O(10)	1.647(14)
Si(1)-O(3)	1.596(14)	Si (1)-O(10)[2]	1.647(14)
Si(1)-O(11)	1.638(14)	Mo(9)-O(21)[2]	2.010(9)
Mo(6)-O(2)[2]	1.971(9)	Mo(3)-O(27)[1]	2.170(6)
Mo(5)-O(3)[2]	2.397(15)	Mo(1)-O(27)[1]	2.186(7)
Mo(6)-O(3)[2]	2.438(13)	Mo(1)-O(29)[1]	2.131(6)
Mo(6)-O(6)[2]	2.036(10)	Mo(2)-O(29)[1]	2.240(7)
Mo(8)-O(7)[2]	2.356(14)	Cu(1)-O(32)[1]	2.417(7)
N(1)-C(30)	1.340(14)	N(2)-C(25)	1.350(13)
N(1)-C(26)	1.365(13)	N(3)-C(10)	1.331(17)
N(2)-C(21)	1.348(15)	N(3)-C(6)	1.366(15)
C(1)-C(2)	1.391(18)	C(3)-C(4)	1.39(3)
C(2)-C(3)	1.38(3)	C(4)-C(5)	1.394(18)
C(5)-C(6)	1.466(17)	C(6)-C(7)	1.386(16)

Symmetry transformations used to generate equivalent atoms: [1]-x+1, -y+1, -z+2; [2] -x, -y+1, -z+1

Table S3. Bond valence calculations for complex **1**.

Complex	Atom	N	$\sum S_{ij}$	Δ
$[(SiMo_{12}O_{40})Cu_6(2,2'\text{-bipy})_6(Mo_6O_{22})]$	Si	4+	3.815	0.185
	Mo1	6+	5.945	0.055
	Mo2	6+	5.983	0.017
	Mo3	6+	6.047	0.047
	Mo4	6+	6.614	0.614
	Mo5	6+	6.773	0.773
	Mo6	6+	6.734	0.734
	Mo7	6+	6.345	0.345
	Mo8	6+	6.479	0.479
	Mo9	6+	6.600	0.600

Table S4. Comparison of photo/electro- performance for complex **1** with other polyoxometalate-based catalysts.

catalyst	Time(min)	CAT[a](%)	Reference
TMSP-1	□90	-	3
TMSP-2	□90	-	3
$[Cu^{II}Lo]$-POM-1	□60	-	4
$[Cu^{II}Lo]$-POM-2	60	-	4
Cu-PW_{12}	□120	-	5
Cu-SiW_{12}	□120	-	5
Cu-PMo_{12}	□120	-	5
Cu-PW_{12}	-	＜20	6
Cu-POMOF	-	＜20	7
Cu-POM	-	＜30	8
Complex **1**	24	33.2	**This work**
[a] represents the CAT at $c(NO_2^-)$=10mM.			

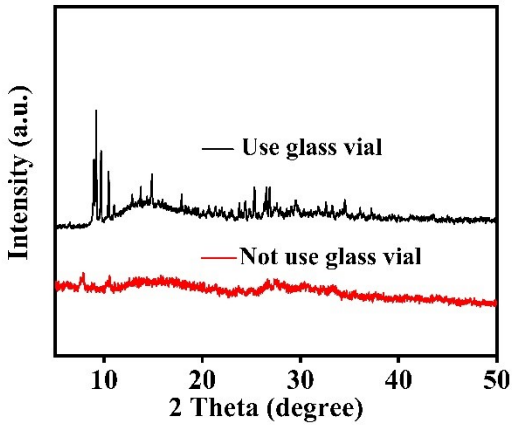

Fig S1. XRD patterns of complex **1** (use glass vials) and green precipitate (not use glass vials).

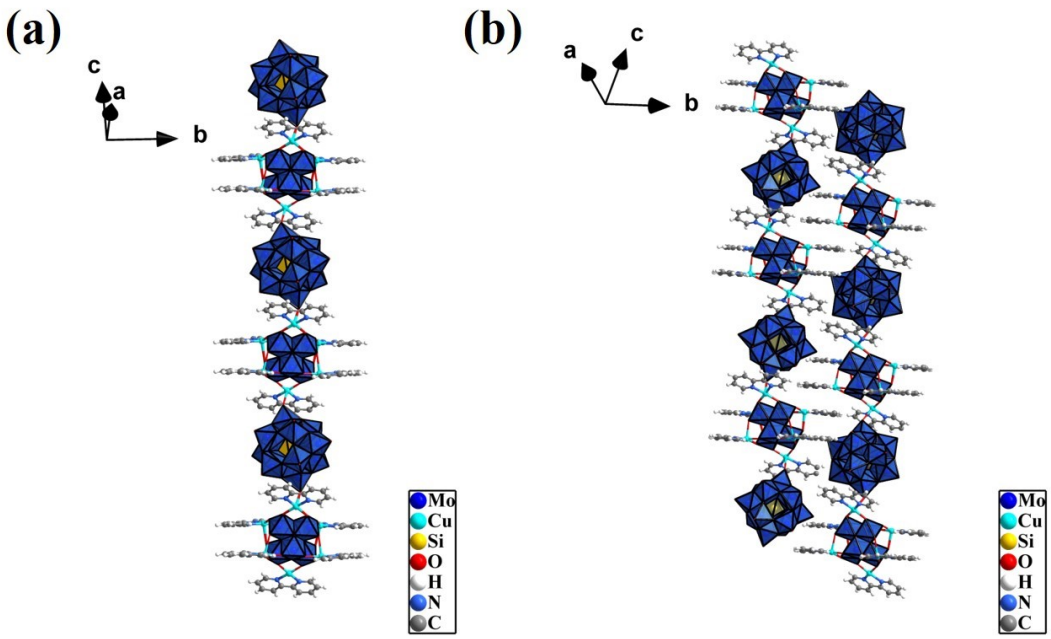

Fig S2. Infinite linear chain (a) and π-π interactions (b) of complex **1.**

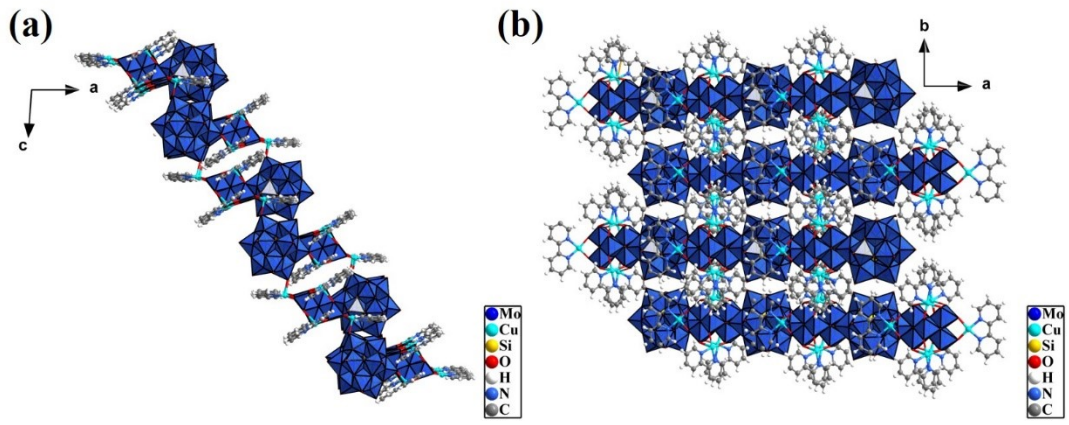

Fig S3. Three-dimensional stacking diagram of complex **1** along the b-axis (b) and the c-axis (c).

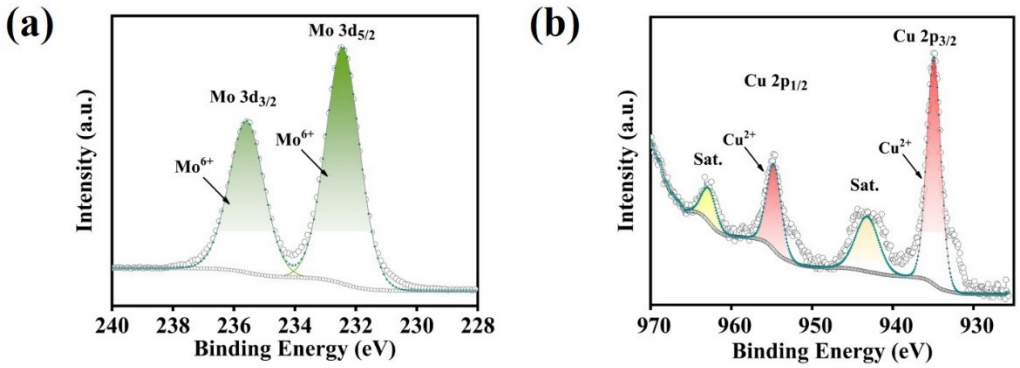

Fig S4. a) Mo 3d and b) Cu 2p XPS spectra of complex **1**.

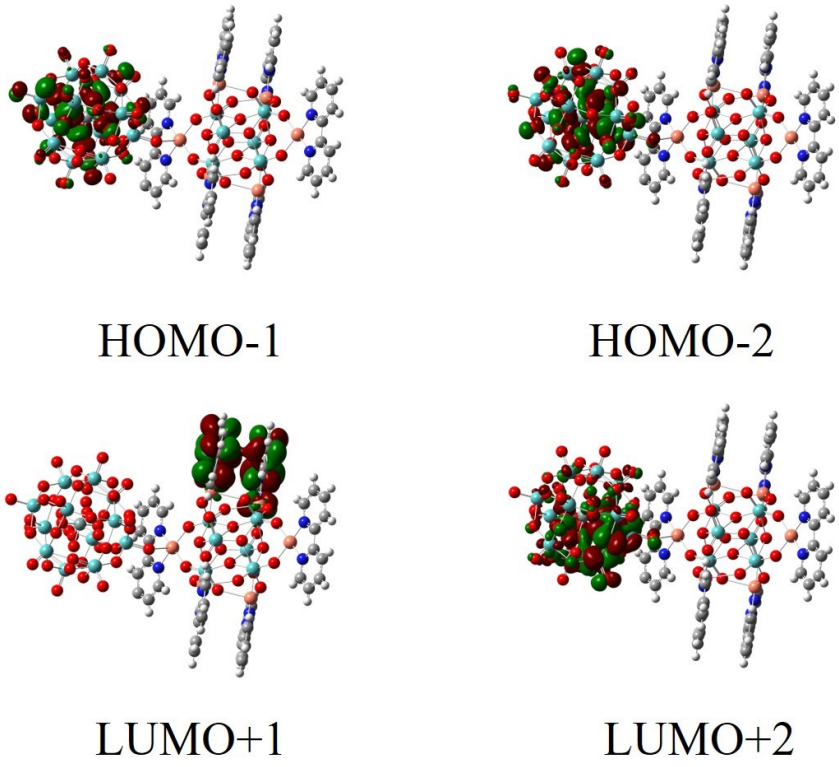

Fig S5. HOMO's and LUMO's of complex **1**.

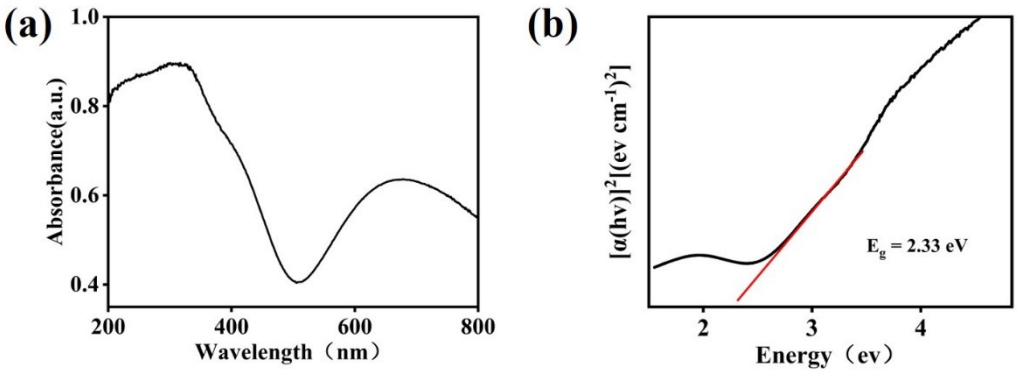

Fig S6. Solid state UV/vis spectrum (a) and diffuse reflection spectra of Kubelka−Munk (K-M) function versus energy (eV) of complex **1**.

Optical Band Gaps

To evaluate the semiconductor behaviors and photocatalytic activities of complex **1**, the diffuse reflection spectra of complex **1** were carried out in the crystalline state at room temperature **(Fig. S3a).** The band gaps (Eg) of complex **1** were obtained from the Kubelka−Munk (K-M) function F vs E, which are estimated to be 2.33 eV (**Fig. S3b).** The band gap values indicate that complex **1** may respond to UV irradiation and have the potential capacity for photocatalytic reactions.[9,10]

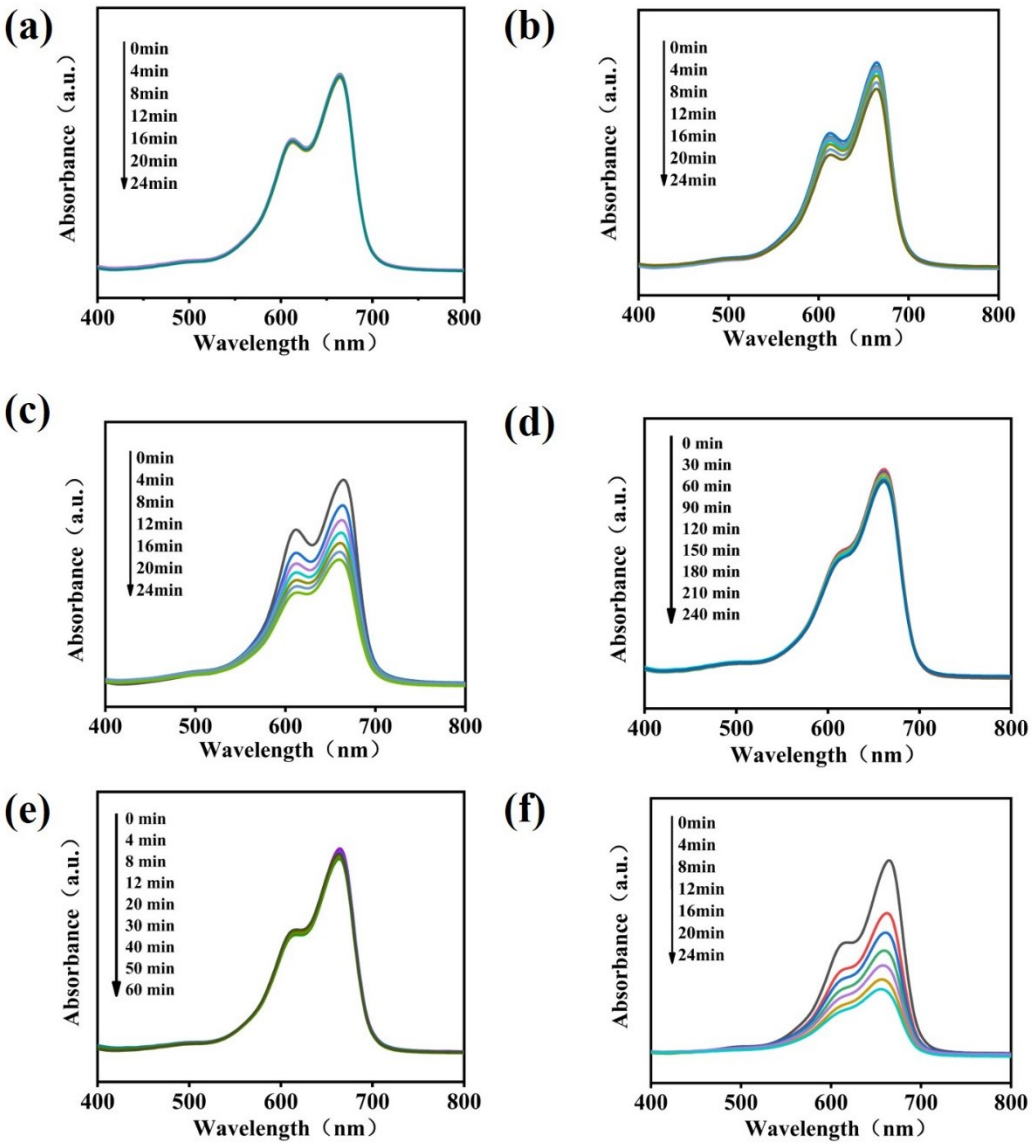

Fig S7. (a) Photocatalytic decomposition rate of the blank MB aqueous solution; Photocatalytic decomposition rate of the MB solution containing (b) complex **1** without H_2O_2; (c) H_2O_2 without complex **1**; (d) complex **1** and H_2O_2 under dark room; (e) complex **1** in an oxygen atmosphere; (f) Cu^{2+}

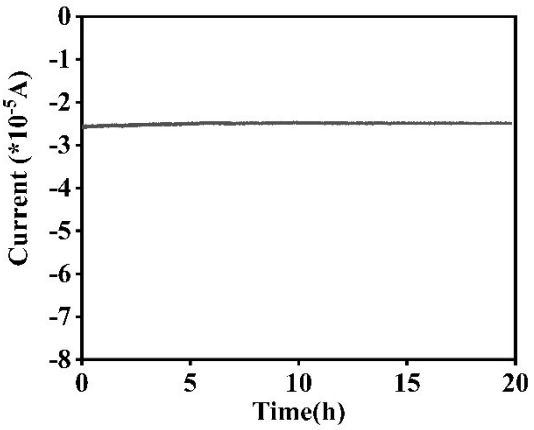

Fig S8. The Amperometric i-t curve of complex **1** in 0.1 M H_2SO_4 + 0.5 M Na_2SO_4 aqueous solution at −0.19V versus SCE.

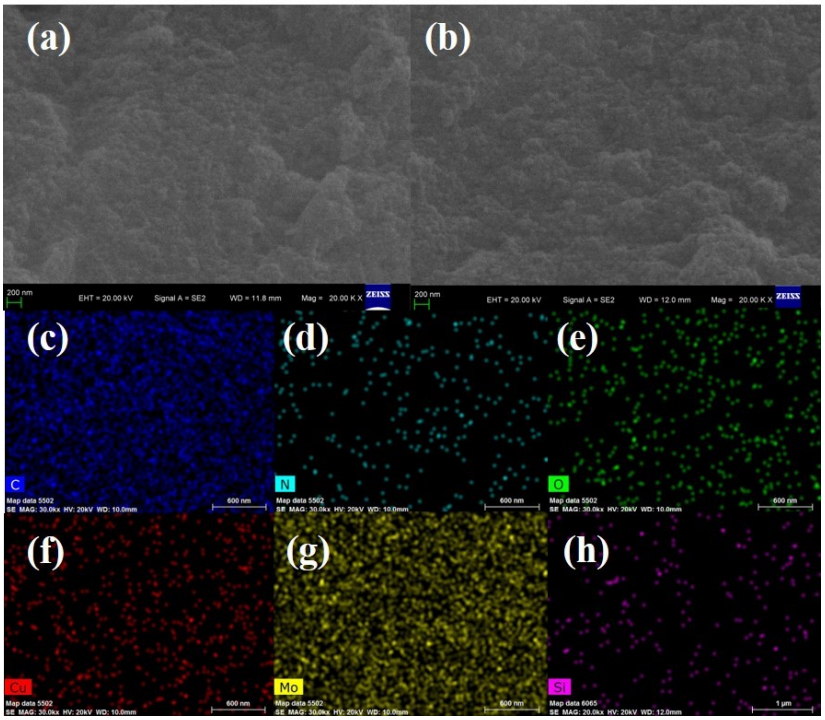

Fig S9. (a-b) SEM images of the substance before and after electrolysis. (c-h) Corresponding elemental mapping images of complex **1**.

References:

1. G.M. Sheldrick. *Acta Cryst.*, 2015, **71**, 3-8.
2. Dolomanov, L.J. Bourhis, R.J. Gildea, J.A.K. Howard and H. Puschmann, *J. Appl. Cryst.*, 2009, **42**, 339-341.
3. J.J. Sun, Y.L. Wang and G.Y. Yang. *CrystEngComm*, 2020, **22**, 8387-8393.
4. L.J. Xu, W.Z. Zhou, L.Y. Zhang, B. Li, H.Y. Zang, Y.H. Wang and Y.G. Li, *CrystEngComm*, 2015, **17**, 3708-3714.
5. S.U. Khan, M. Akhtar, F.U. Khan, J. Peng, A. Hussain, H.F. Shi, J. Du, G. Yan and Y.G. Li, *J. Coord. Chem.*, 2018, 71, 16-18.
6. Y. Hou, Y. Niu, C.J. Zhang, H.J. Pang and H.Y. Ma, *J. Chem. Sci.*, 2017, **129**, 1639-1645.
7. W.L. Sun, S.B. Li, H.Y. Ma, H.J. Pang, L. Zhang and Z.F. Zhang, *RSC Adv.*, 2014, **4**, 24755-24761.
8. J.W. Zhao, D.Y. Shi, L.J. Chen, P.T. Ma, J.P. Wang, J. Zhang and J.Y. Niu, *Cryst. Growth Des.*, 2013, **13**, 4368-4377.
9. T. Wen, D.X. Zhang and J. Zhang. *Inorg. Chem.*, 2013, **52**, 12-14.
10. W.Q. Kan, B. Liu, J. Yang, Y.Y. Liu and J.F. Ma, *Cryst. Growth Des.*, 2012, **12**, 2288-2298.